International Applied Mechanics, Vol. 43, No. 5, 2007

INELASTIC DEFORMATION OF FLEXIBLE CYLINDRICAL SHELLS WITH AN ELLIPTIC HOLE

I. S. Chernyshenko, E. A. Storozhuk, and F. D. Kadyrov UDC 539.374

The elastoplastic state of isotropic homogeneous cylindrical shells with elliptic holes and finite deflections under internal pressure is studied. Problems are formulated and numerically solved taking into account physical and geometrical nonlinearities. The distribution of stresses (displacements, strains) along the boundary of the hole and in the zone of their concentration is analyzed. The data obtained are compared with the numerical solutions of the physically nonlinear, geometrically nonlinear, and linear problems. The stress–strain state of cylindrical shells in the neighborhood of the elliptic hole is analyzed with allowance for nonlinear factors

Keywords: nonlinear problem, cylindrical shells, stress concentration, elliptic hole, internal pressure, plastic strains, finite deflections

Introduction. The distribution of stresses (strains, displacements) in isotropic and anisotropic, simply and multiply connected structural members (shells, plates) has mostly been studied for the elastic range of deformation [1, 3, 5–7, 9, 10]. The major results have been obtained in solving static linear elastic problems for thin and nonthin shells with curvilinear (circular, elliptic, etc.) holes (cutouts) under surface and edge loads. The use was made of theories of shells based on hypotheses on structural members made of traditional metallic and advanced composite materials. To formulate and solve problems of this class, variational, numerical, and analytic methods were used.

Physically nonlinear problems that deal with nonlinear elastic, plastic, and creep strains in members (isotropic or orthotropic) of shell structures of positive or zero Gaussian curvature with curvilinear holes are solved in [4, 6, 7, 12, 14, etc.]. The distribution of stress/strain components around an elliptic hole is studied in [3, 5–8, 11, 17] by solving boundary-value problems and taking into account the physical nonlinearity of materials (metals, composites).

Also of interest are two-dimensional nonlinear problems of stress concentration around elliptic (noncircular) holes in isotropic cylindrical shells with both physical and geometrical (finite, large deflections) nonlinearities. Such studies are even more important in connection with calculations for high levels of loads (surface pressure, axial forces, edge forces, moments).

The present paper discusses results, obtained by the method developed in [2] and presented in support of its applications [14, 16, 18], from a numerical analysis of the elastoplastic stress–strain state around an elliptic hole in a flexible cylindrical shell under a surface load. We will examine the influence of physical (plastic deformations) and geometrical (finite deflections) nonlinearities on the distribution of stresses and strains in the zone of their concentration in a shell under internal pressure of given magnitude.

1. Let us analyze the elastoplastic state of a thin isotropic cylindrical shell (of radius R, thickness h = const) with an elliptic hole (a and b are the ellipse semiaxes). The shell is subject to a surface load $\{p\} = \{p_1, p_2, p_3\}^T$ and an edge load $\{m\} = \{T_b, S_b, Q_b, M_b\}^T$. Assume that high loads cause plastic strains (structural properties, mechanical characteristics, and stress–strain curve $(\sigma - \varepsilon)$ of the material are known) and deflections (along the normal to the shell near the hole) commensurable with the thickness of the shell.

S. P. Timoshenko Institute of Mechanics, National Academy of Sciences of Ukraine, Kyiv. Translated from Prikladnaya Mekhanika, Vol. 43, No. 5, pp. 46–54, May 2007. Original article submitted February 7, 2006.

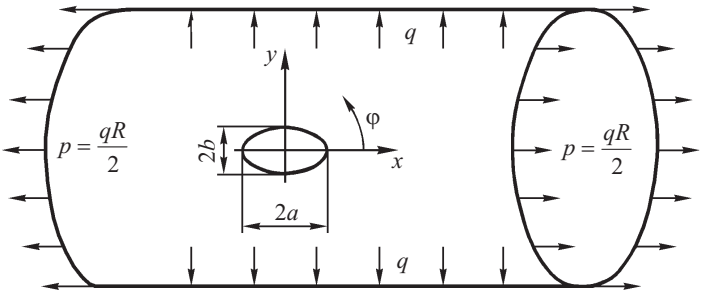

Fig. 1

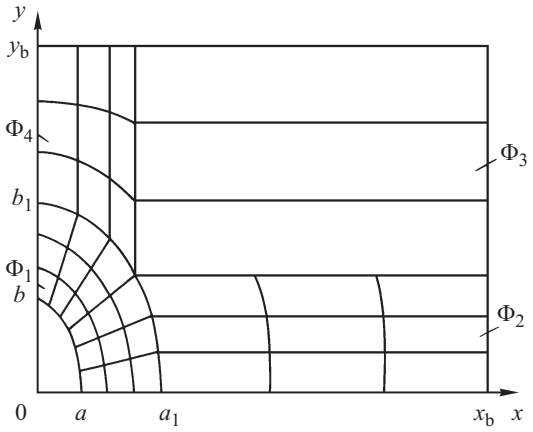

Fig. 2

The mid-surface of the shell (Fig. 1) is described in a Cartesian coordinate system (x, y) with the Ox-axis directed along the semiaxis a (in the longitudinal direction of the cylinder). The boundary of the elliptic hole is described by the parametric equation

$$x = a\cos\varphi, \qquad y = b\sin\varphi, \tag{1}$$

where φ is the angle of the elliptic coordinate system.

In the general case [2, 15] of an arbitrary thin shell described in a coordinate system not aligned with the lines of principal curvature, the geometrical equations are derived from the theory of flexible shells (second-order theory of shells) and the physical equations from the flow theory with isotropic hardening.

To derive the governing system of equations [2, 15] that describes the elastoplastic state of a shell with an elliptic hole and finite deflections, the virtual-displacement principle and approximate methods are used. The method for approximate solution of nonlinear problems used here is based on the incremental loading procedure. The doubly nonlinear problem posed will be solved by sequentially applying the modified Newton–Kantorovich method (geometrically nonlinear problem), the method of additional stresses (physically nonlinear problem), and the finite-element method (FEM) and using a matrix notation for the equations.

After linearization and FEM discretization of the variational equation, we obtain a governing system of algebraic equations, which can be represented in the following form for the nth step of loading [2]:

$$[M]\{\Delta q\} = \{\Delta V\},$$

$$[M] = [M_0] + [M_\alpha] + [M_\sigma], \qquad \{\Delta V\} = \{\Delta P\} - \{\Delta N\} + \{\Delta\Phi\}, \tag{2}$$

where $[M_0]$ is the incremental stiffness matrix for linearly elastic shells; $[M_\alpha]$ and $[M_\sigma]$ are the influence matrices for the initial angles of rotation of the tangents to the coordinate lines and for stresses; $\{\Delta q\}$ is the global column vector of increments of nodal degrees of freedom (nodal variables); $\{\Delta P\}$, $\{\Delta N\}$, and $\{\Delta\Phi\}$ are the vectors of loads, nonlinearities, and residues of the equilibrium equations at the end of the previous step of loading. Note that the stiffness matrices are calculated using the matrix $[D]$ defined by the elastic characteristics of the shell.

To solve specific nonlinear problems for shells, Eqs. (2) with (1) should be supplemented with boundary conditions at the external and internal edges (boundaries of the domain of interest).

2. The method and algorithm for solving the nonlinear problems formulated have been implemented in a software package [2], which makes it possible to analyze the inelastic stress–strain state of flexible cylindrical shells with an elliptic hole under a prescribed load.

The method was validated by comparing the numerical solution of a linear elastic problem [8] and experimental data [18] for a cylindrical shell with the following characteristics: $\kappa = r_0 / \sqrt{Rh} = 1.667$, $r_0 = (a+b)/2$, $b = 2a$, $E = 70$ GPa, $\nu = 0.4$.

TABLE 1

φ	ξ	σ^*_φ (LP)				
		$a^* = 1/2$	$a^* = 2/3$	$a^* = 1$	$a^* = 3/2$	$a^* = 2$
0	0.5 –0.5	2540 2847	2408 3889	2794 5933	4306 8863	6457 11490
π/14	0.5 –0.5	2646 2744	2573 3739	2974 5661	4189 8268	5610 10380
π/4	0.5 –0.5	3495 1651	3662 1946	3760 2327	3548 2499	3255 2404
3π/7	0.5 –0.5	3985 –85	3493 –1099	2986 –2572	2668 –3812	2459 –4574
π/2	0.5 –0.5	3993 –153	3339 –1563	2808 –3206	2528 –4539	2338 –5340

It is assumed that the hole is free from forces and that the load (axial tension; $P/h = 9.81$ MPa) is uniformly distributed along the edge x = const. The following boundary conditions are prescribed on the boundary of the hole [6]:

$$\widetilde{T}_\sigma = \widetilde{T}_{\sigma\tau} = 0, \quad M_\sigma = 0, \quad \widetilde{Q}^*_\sigma = 0. \tag{3}$$

The stress state is momentless far from the hole ($x = x_b$):

$$\widetilde{T}_{\sigma\tau} = \widetilde{Q}^*_\sigma = 0, \quad M_\sigma = 0, \quad \widetilde{T}_\sigma = P. \tag{4}$$

Symmetry conditions hold on the boundaries $x = 0$, $y = 0$, and $y = y_b = R/(\pi/2)$:

$$u_\sigma = 0, \quad \varphi_\sigma = 0, \quad \widetilde{T}_{\sigma\tau} = \widetilde{Q}^*_\sigma = 0. \tag{5}$$

The displacements, strains, and stresses at nodes of the mesh and points throughout the thickness calculated in solving the test problem with conditions (3)–(5) are summarized in tables. The stress distribution ($K_\sigma = \sigma_\varphi h/P$) along the elliptic boundary is shown by plots [8, 18], which are indicative of the efficiency of the numerical method and quite accurate solution of the problem for a shell of complex geometry.

Note that the complete solution has been obtained in view of the condition

$$(||\Delta q||^i_n / ||q||^i_n) \le \delta \qquad (\delta \le 10^{-2}),$$

where q is the deflection (characteristic quantity) at a given point (node) in the nth approximation; Δq is the difference of the values of this quantity in the nth and $(n-1)$th approximations; δ is prescribed accuracy.

3. We have solved the following problems for shells under internal pressure $q = q_0 \cdot 10^5$ Pa: (i) linear elastic problem (LP) for $q_0 = 1$ and (ii) nonlinear elastic problems (PNP, GNP, and PGNP) for $q_0 = 10$.

For reasons of geometrical and force symmetry, the problems can be solved in the domain (Σ) bounded by the hole boundary and the lines $x = 0$, $x = x_b$; $y = 0$, $y = y_b$ (Fig. 2).

The numerical results discussed below have been obtained for a cylindrical shell with the following geometry:

$$\eta = \frac{R}{h} = 400, \quad r^* = \frac{2r_0}{h} = 30, \quad r_0 = \frac{a+b}{2}, \quad a^* = a/b = 1/2,\ 2/3,\ 1.0,\ 3/2,\ 2.0 \tag{6}$$

TABLE 2

φ	w^* (LP)				
	$a^* = 1/2$	$a^* = 2/3$	$a^* = 1$	$a^* = 3/2$	$a^* = 2$
0	2.954	1.120	0.0735	0.662	1.953
π/14	2.994	1.211	0.2047	0.807	2.105
π/4	3.233	1.927	1.3990	2.388	3.988
3π/7	3.245	2.427	2.5940	4.414	6.715
π/2	3.232	2.469	2.7260	4.663	7.063

TABLE 3

NP	φ	w^*				
		$a^* = 1/2$	$a^* = 2/3$	$a^* = 1$	$a^* = 3/2$	$a^* = 2$
PNP	0	3.518	1.599	0.323	1.229	3.643
	π/4	4.132	3.368	4.284	9.257	15.980
	π/2	4.120	4.083	6.705	15.980	28.590
GNP	0	1.138	0.8742	0.6912	0.7443	0.8987
	π/4	1.195	1.076	1.068	1.340	1.652
	π/2	1.206	1.261	1.599	2.299	2.958
PGNP	0	1.320	1.106	1.023	1.164	1.385
	π/4	1.361	1.310	1.495	1.962	2.456
	π/2	1.350	1.473	2.006	2.970	3.890

made of an AMg-6 material ($E = 70$ GPa, $\nu = 0.3$–0.5, $\sigma_{\text{п}} = 140$ MPa, $\varepsilon = 0.002$, $\sigma_{\text{т}} = 165$ MPa), and subjected to internal pressure $q = 10^6$ Pa.

It is assumed that the hole is closed with a plug that transmits only the shearing forces $Q_{\text{b}} = qr_0 / 2$ to the boundary of the hole.

At a sufficient distance from the hole, the stress state is momentless:

$$T_{\text{b}} = qR / 2 \quad \text{on the boundary} \quad x = x_{\text{b}},$$

$$T_{\text{b}} = qR \quad \text{on the boundary} \quad y = y_{\text{b}}. \tag{7}$$

The process of loading was divided into 10 steps to solve physically nonlinear problems for the shell (6) with (7) (elastoplastic strains) and into 20 steps if $a/b = 3/2$; 2.0 and into 10 steps if $a/b = 1/2$; 2/3; 1.0 to solve geometrically nonlinear problems (finite deflections).

TABLE 4

NP	φ	σ_φ^*				
		$a^* = 1/2$	$a^* = 2/3$	$a^* = 1$	$a^* = 3/2$	$a^* = 2$
PNP	0	1698 / 1807	1689 / 1955	1733 / 2235	1932 / 2915	2429 / 4080
	π/4	1848 / 1492	1907 / 1373	1957 / 581	1969 / 3	1877 / –97
	π/2	1840 / –840	1762 / –1592	1802 / –1905	1966 / –2203	2146 / –2478
GNP	0	2377 / 2181	2665 / 2647	3461 / 3721	4960 / 5491	6627 / 7270
	π/4	2560 / 1783	2779 / 1963	2878 / 2208	2822 / 2360	2694 / 2391
	π/2	2844 / 687	2393 / –81	2126 / –904	2144 / –1412	2238 / –1605
PGNP	0	1630 / 1609	1714 / 1713	1845 / 1852	2019 / 2040	2247 / 2279
	π/4	1647 / 1512	1702 / 1557	1737 / 1584	1723 / 1565	1697 / 1508
	π/2	1699 / 609	1585 / –141	1538 / –923	1534 / –1322	1529 / –1328

The domain (Σ) is covered with an irregular mesh of curvilinear fragments Φ_i $(i = \overline{1, 4})$ each regularly divided into finite elements (FEs). The optimal mesh is selected by solving test problems for elastic shells with an elliptic hole and comparing solutions obtained from different meshes. Five FE meshes have been tested; the optimal mesh for the fragments in Fig. 2 consists of 245 FEs.

The tables and figures here show some of the values of displacements, strains, and stresses in a cylindrical shell with an elliptic hole obtained in solving linear and nonlinear problems.

Table 1 collects the values of the maximum stresses $\sigma_\varphi = \sigma_\varphi^* \cdot 10^5$ Pa along the hole boundary $(0 \le \varphi \le \pi/2)$ on the outside and inside surfaces $(\xi = \gamma / h = \pm 0.5)$ for $a^* = 1/2, 2/3, 3/2, 2$. The dependence of relative deflections $(w^* = w/h)$ on the angle φ $(\xi = 0)$ for a shell with a circular hole $(a^* = 1)$ is shown in Table 2. The components of the displacement vector (u, v, w), strain tensor (e_{ij}), and stress tensor (σ_{ij}) have been calculated at the edge and near the hole by solving PNP, GNP, and PGNP for $q_0 = 2$.

Table 3 summarizes the values of displacements w^* calculated at three points $(\varphi = 0, \pi/4, \pi/2)$ of the hole boundary for different aspect ratios a^*. Table 4 gives the maximum (circumferential) stresses σ_φ^* on the outside (numerator) and inside (denominator) surfaces $(\xi = \pm 0.5)$ at three points $(\varphi = 0, \pi/4, \pi/2)$ of the hole boundary.

Figures 3–7 demonstrate how the stress concentration factor $K_\varphi = \sigma_\varphi h / qR$ varies along the hole boundary in the mid-surface of the shell $(\xi = 0)$ with an elliptic and circular hole. Curves *1*, *2*, *3*, and *4* correspond to LP, PNP, GNP, and PGNP, respectively.

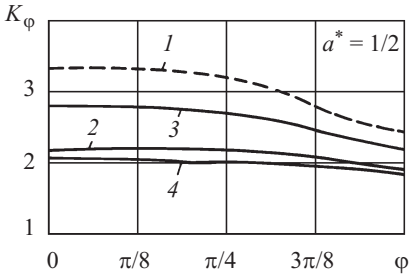

Fig. 3

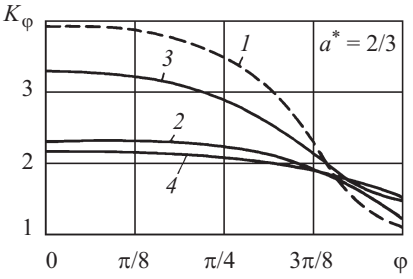

Fig. 4

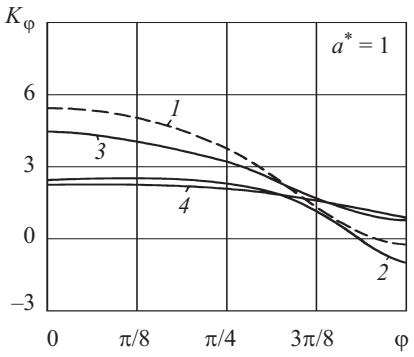

Fig. 5

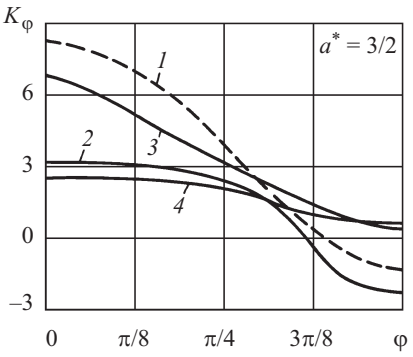

Fig. 6

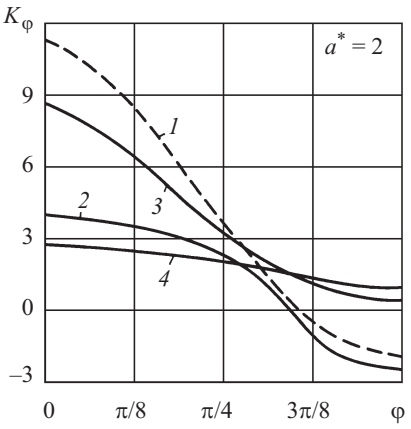

Fig. 7

An analysis of the results shows that for $a^* > 1$ as well as $a^* = 1$ (circular hole), the most critical is the section on the hole boundary at the point $\varphi = 0$ on the outside surface where the stresses σ_φ peak. As the aspect ratio decreases ($a^* < 1$), the stresses in the section $\varphi = 0$ are redistributed throughout the thickness and their maximum shifts from the point $\varphi = 0$ to the point $\varphi = \pi/2$. Therefore, when $a = 1/2$, the most critical section is on the hole boundary at the point $\varphi = \pi/2$ on the outside surface. This effect is due to the fact that internal pressure generates not only a surface load, but also axial tensile forces $T_b = qR/2$ at the edges $x = x_b$. Maximum stresses occur at the point $\varphi = 0$ on the hole boundary under surface loading and at the point $\varphi = \pi/2$ under axial loading. The contribution of each type of loading to the total stress–strain state depends on the aspect ratio of the elliptic hole; therefore, as the parameter a^* changes, the stresses are redistributed throughout the thickness and on the boundary of the hole.

The maximum deflection is observed at the point $\varphi = \pi/2$ of the hole boundary when $a^* = 2/3; 3/2; 2$ (as well as when the hole is circular) and shifts from the point $\varphi = \pi/2$ to the point $\varphi = 0$ when $a^* \le 1/2$. The cause of this effect is the same as for stresses.

In the PNP for $a^* = 1/2$, 2/3, 1, 3/2, and 2, the maximum stress is less by 54, 50, 62, 67, and 64% and the maximum deflection is greater by a factor of 1.3, 1.7, 2.5, 3.4, and 4.1, respectively, than in the LP.

In the GNP for the same values of a^*, the maximum stress is less by 29, 31, 37, 38, and 37% and the maximum deflection is less by 63, 49, 41, 51, and 58%, respectively, then in the LP.

In the PGNP for $a^* = 1/2$, 2/3, 1, 3/2, and 2, the maximum stress is less by 57, 56, 69, 77, and 80%, respectively, than in the LP, different by 40, 37, 50, 6, and 69% than in the PNP and by 6, 12, 17, 30, and 44% from that in the GNP.

As the aspect ratio (a^*) increases, the maximum stress concentration factor increases from $K_\varphi = 4.99$ at $a^* = 1/2$ to $K_\varphi = 14.36$ at $a^* = 2$ in the LP; from $K_\varphi = 2.31$ at $a^* = 1/2$ to $K_\varphi = 5.1$ at $a^* = 2$ in the PNP; from $K_\varphi = 3.56$ at $a^* = 1/2$ to $K_\varphi = 9.09$ at $a^* = 2$ in the GNP; and from $K_\varphi = 2.12$ at $a^* = 1/2$ to $K_\varphi = 2.85$ at $a^* = 2$ in the PGNP. Thus, nonlinearities greatly affect the stress–strain state of cylindrical shells with an elliptic hole.

REFERENCES

1. A. N. Guz, A. G. Makarenko, and I. S. Chernyshenko, *Strength of the Structure of Solid Rocket Motors* [in Russian], Mashinostroenie, Moscow (1980).
2. A. N. Guz, E. A. Storozhuk, and I. S. Chernyshenko, "Physically and geometrically nonlinear static problems for thin-walled multiply connected shells," *Int. Appl. Mech*., **39**, No. 6, 679–687 (2003).
3. A. N. Guz, I. S. Chernyshenko, and K. I. Shnerenko, "Stress concentration near openings in composite shells," *Int. Appl. Mech*., **37**, No. 2, 139–181 (2001).
4. A. L. Kravchuk, E. A. Storozhuk, and I. S. Chernyshenko, "Stress distribution in flexible cylindrical shells with a circular cut beyond the elastic limit," *Int. Appl. Mech*., **24**, No. 12, 1179–1183 (1988).
5. V. A. Maksimyuk and I. S. Chernyshenko, "Mixed functionals in the theory of nonlinearly elastic shells," *Int. Appl. Mech*., **40**, No. 11, 1226–1262 (2004).
6. A. N. Guz, I. S. Chernyshenko, V. N. Chekhov, et al., *Theory of Thin Shells with Holes*, Vol. 1 of the five-volume series *Methods of Shell Design* [in Russian], Naukova Dumka, Kyiv (1980).
7. A. N. Guz, A. S. Kosmodamianskii, V. P. Shevchenko, et al., *Stress Concentration*, Vol. 7 of the 12-volume series *Mechanics of Composite Materials* [in Russian], A.S.K., Kyiv (1998).
8. V. P. Mulyar, E. A. Storozhuk, and I. S. Chernyshenko, "Elastoplastic state of thin-walled cylindrical shells with an elliptic hole in the lateral wall," *Prikl. Mekh*., **33**, No. 6, 62–68 (1997).
9. G. N. Savin, *Stress Distribution around Holes* [in Russian], Naukova Dumka, Kyiv (1969).
10. V. A. Salo, *Static Boundary-Value Problems for Shells with Holes* [in Russian], Nats. Tekhn. Univ. "KhHPI," Kharkov (2003).
11. E. A. Storozhuk, I. S. Chernyshenko, and V. L. Yaskovets, "Elastoplastic state of spherical shells in the region of an elliptical hole," *Int. Appl. Mech*., **25**, No. 7, 667–672 (1989).
12. E. N. Troyak, E. A. Storozhuk, and I. S. Chernyshenko, "Elastoplastic state of a conical shell with a circular hole on the lateral surface," *Int. Appl. Mech*., **24**, No. 1, 65–70 (1988).
13. I. A. Tsurpal and N. G. Tamurov, *Design of Multiply Connected Laminated Nonlinear Elastic Plates and Shells* [in Russian], Vysshaya Shkola, Kyiv (1977).
14. I. S. Chernyshenko and E. A. Storozhuk, "Inelastic deformation of flexible cylindrical shell with a curvilinear hole," *Int. Appl. Mech*., **42**, No. 12, 1414–1420 (2006).
15. V. P. Mulyar, "On the stress distribution in a spherical shell with an off-center curvilinear hole," *Int. Appl. Mech*., **42**, No. 1, 98–102 (2006).
16. K. I. Shnerenko and V. F. Godzula, "Stress state of a cylindrical composite panel weakened by a circular hole," *Int. Appl. Mech*., **42**, No. 5, 555–559 (2006).
17. E. A. Storozhuk and I. S. Chernyshenko, "Physically and geometrically nonlinear deformation of spherical shells with an elliptic hole," *Int. Appl. Mech*., **41**, No. 6, 666–674 (2005).
18. R. S. Tennyson, D. K. Roberts, and D. Zimcik, "Analysis of the stress distribution around unreinforced cutouts cylindrical shells under axial compression," *NRS*, *NASA. Ann. Prog. Rept*., UTJAS, 118–129 (1968).